Asian Journal of Physics
Vol. 32, Nos 1 & 2 (2023) 11-20
Available on: www.asianjournalofphysics.com

ap

Systematic study of the effect of small-molecules on the low-frequency Raman spectrum of water

Julian Hniopek[a,b], Julian Plitzko[a,b], James Carriere[c], Peter Vogt[d], Michael Schmitt[a] and Jürgen Popp[a,b]

[a]*Institute for Physical Chemistry and Abbe Center of Photonics*, *Friedrich Schiller University Jena*, *Helmholtzweg 4*, *07743*, *Jena*, *Germany.*

[b]*Leibniz Institute of Photonic Technology* (*IPHT*), *Member of Leibniz Research Alliance - Leibniz Health Technologies and of the Leibniz Centre for Photonics in Infection Research* (*LPI*), *Albert-Einstein-Str. 9*, *07745*, *Jena, Germany.*

[c]*Coherent, Inc.- Ondax, 850 E. Duarte Rd*., *Monrovia*, *CA 91016, United States of America.*

[d] *Coherent Shared Services B.V*., *Dieselstrasse 5b*, *64807 Dieburg*, *Germany.*

Low-frequency Raman, which is Raman spectroscopy focused onto the wavenumber region below 100 cm^{-1}, has gained considerable interest over the last decades due to better availability of instrumentation. However, so far it has mostly been restricted to the investigation of solid structures, where clear features are present. For dissolved, especially aqueous, samples, the use of low-frequency Raman is hindered by a lack of sharp features and strong background signal of water. Nevertheless, by influencing hydrogen bonding, dissolved species affect the low-frequency spectrum of water. To use these changes analytically, a systematic knowledge of the effects is necessary. Therefore, we present a systematic study of the effect of small molecules ranging from apolar to salts on the low-frequency spectrum of water. Changes to the hydrogen-bonding associated vibrations could be detected for all molecules that correlate well with their physicochemical properties. Furthermore, by employing two-dimensional correlation spectroscopy, it could be revealed that the changes to the hydrogen bonding environment often follow more complicated complex mechanisms, which helps to understand the mechanism behind hydrogen bonding in heterogenous systems. The present study is a first step to understand the low-frequency spectra of aqueous solutions.

Keywords: Low-frequency Raman, THz-spectroscopy, 2D correlation spectroscopy, hydrogen-bonding.

1 Introduction

Low-frequency vibrational spectroscopy are techniques that observe vibrational transitions with energies lower than ca. 100 cm^{-1}, to achieve understanding about structural properties of matter [1]. Unlike traditional vibrational spectroscopic techniques, low-frequency vibrational spectroscopy is capable of providing additional information about the low-frequency vibrations of materials, making it a valuable tool for the study of weakly bound systems, liquids, and soft materials [1,2]. However, it has been a rather underdeveloped field for a long time [3,4]. This was majorly caused by experimental difficulties in observing those transitions both *via* direct excitation, i.e. THz-spectroscopy and indirect observation *via* inelastic scattering processes, i.e. low-frequency (THz)-Raman.

For THz-spectroscopy, the major obstacle to the observation of these low energy transitions was the availability of both sources and especially detectors for radiation in the THz frequency region. Systems that overcome this obstacle have only been widely available for roughly three decades.

While the low-frequency Raman is theoretically much easier to realize from a technical standpoint, as no direct generation or detection of low-frequency radiation is necessary, it has for a long time suffered

Corresponding author
e mail: juergen.popp@uni-jena.de (Jürgen Popp)

from the need of complicated experimental setups. This is mainly due to the fact that suppression of elastically scattered signal as well as wavelength stability and spectral bandwidth of the excitation source become more and more important for low-frequency detection, since the detected photon wavelength gets closer to the excitation wavelength [5]. Furthermore, to record a high-quality spectrum in the low-frequency region, relatively high spectral resolutions are necessary to achieve a number of points sufficient to recover the band shapes.

All these points lead to the fact that for the longest time, low-frequency Raman spectroscopy could only be carried out using triple-monochromator systems [6], which are expensive, difficult to set up and maintain, and need constant tuning to changing environmental parameters. This has only changed in the last decade with the availability of ultra-high fidelity bandpass and notch filters based on volume holographic grating technology [7]. These filters enable compact, cheap, and stable setups for low-frequency Raman, that have majorly contributed to an increase in research output in this area [8].

Low-frequency Raman spectroscopy is an established tool in solid-state physics [9-11], material characterization [12], and over the last decades has also been developed as a major tool for process analysis especially in the pharmaceutical industry [3,13].

Most of these applications deal with solid-state materials, where defined geometric arrangements of atoms exist. These defined geometries lead to the presence of relatively sharp signals that look similar to signals observed in the classic fingerprint spectrum. In such systems, changes in geometric arrangement, e.g., a different crystal structure, different enantiomers etc., can easily be observed by changes in the band structure of the low-frequency region. This easy access to information about solid-state arrangement explains the popularity especially in the pharmaceutical sciences [14], where a small difference, such as a different enantiomer or polymorph might have catastrophic effects on the patient.

However, while the solid-state applications have been developed comparatively far over the last decades, applications to systems that are dissolved or surrounded by liquid are still few and far between. This especially means, that application to biological systems, which usually contain at least water, remained basically unresearched. In such systems, no fixed geometric arrangement of atoms is present, as molecules / species are free to rotate both internally and externally. As a consequence, no clear band structure is visible. Only a broad signal arises from a combination of quasi-elastic scattering and a high number of distinct vibrational states spaced closer than the natural linewidth, i.e., are non-resolvable.

For biological applications, or more general application to aqueous systems, it is important to note, that this broad signal is also detectable for pure water with relatively high scattering efficiency [2]. Contrary to fingerprint Raman spectroscopy, water cannot be viewed as a non-disturbing substance for low-frequency Raman spectroscopy and the water signal often completely obfuscates the signals from dissolved species. This means, that direct observation of species dissolved or surrounded by water is not easily possible.

On the other hand, the signals arising from water could be used to indirectly characterize the dissolved molecules by the interaction they have with water. Since the low-frequency band of water is influenced by the type and strength of hydrogen-bonding between the water molecules, any changes to this intermolecular force will also change its low-frequency spectrum [15]. Therefore, indirect observations about dissolved species can be made, i.e., how they interact with the surrounding water environment and thus how polar they are. However, to get information from such experiments it is necessary to systematically characterize the influence of molecules on the low-frequency Raman band structure of water, which to the best of our knowledge has not been done so far.

In the present study, we therefore investigated the low-frequency Raman spectrum of a number of small molecules ranging from relatively apolar to polar substances that were dissolved in or mixed with water in concentrations between 0 and 1 mol/L. Hereby, we could systematically analyze the effect of each of the substances on the low-frequency spectrum of water and correlate them with known physicochemical

properties and provide a first systematic overview of this effect that could be used to indirectly observe dissolved substance in aqueous environments.

2 Experimental

2.1 Spectroscopic methods

All Raman spectroscopic measurements were performed using a Ondax (now part of Coherent Corp., Saxonburg PA, United States of America) TR PROBE excited at 808 nm coupled to a Kaiser (Ann Arbor, MA, United States of America) RXN1 spectrometer, equipped with a volume holographic grating and multi-line detector. Measurements were performed in glass mass spectrometry vials *via* a vial adapter provided with the Ondax instrument in back-scattering geometry.

Using high-performance ultra-low-bandwidth notch and bandpass filters (Fig 1) the system enables collecting Raman spectra up to ca. ±5 cm^{-1} to the Rayleigh line in a straight-forward manner. Using the fixed-grating spectrometer of the RXN1 setup, collection of Raman signal in the range between –100 and +2500 cm^{-1} (Anti-Stokes side) is possible. To ensure wavelength and intensity stability of the multi-line detection setup, the spectrometer was calibrated against neon and white light-emission standards.

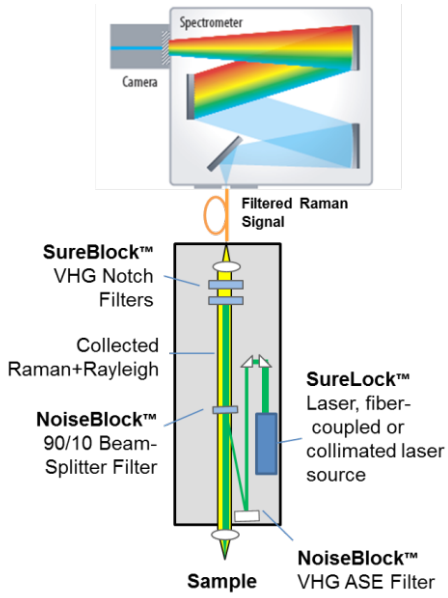

Fig 1. Schematic drawing of the Coherent TR PROBE eetup used in this study.

2.3 Data processing

The data pre-processing was done using R (4.2.2) with in-house developed scripts and the software packages Peaks & nls.

To remove any variations in focus depth and laser fluctuations, first the spectra were normalized using the intrinsic luminescence signal of the glass vial, that presents itself in a broad peak between 1000 and 2000 cm^{-1}. Within a single batch of vials, this signal has been found to be very reproducible and thus suitable as an internal standard for normalization. For further evaluation, only the low-frequency part of the spectrum, i.e., below 300 cm^{-1} was used.

Two-dimensional correlation spectroscopy (2DCOS) was performed using in-house developed methods that have been described in detail elsewhere [16]. In all cases, the whole range of concentrations was

used for the generation of the 2DCOS maps. As reference spectra, the pure water spectra of each measurement series were utilized.

3 Results and Discussion

3.1 Low-frequency Raman spectra

In this study, series of 7 small molecules dissolved in water in concentrations between 0 and 1 mol/L were prepared and investigated using low-frequency Raman spectroscopy. The small molecules used were all readily dissolvable in water and span a range of different chemical properties that could influence the water environment differently: A relatively apolar solvent (tetrahydrofurane), a polar aprotic solvent (acetone), a zwitterionic structure (glycine), a very polar solid (D-glucose), a weak acid (acetic acid) and strong acid (hydrochloric acid) as well as a salt with very high ion strength (sodium chloride). Due to the broad range of physicochemical properties covered, these molecules should provide a good overview of possible changes to the structure of the low-frequency band of water upon addition of another component. Figure 2 shows the resulting low-frequency spectra in concentrations of 0, 0.2, 0.4, 0.6, 0.8 and 1M, as well as the resulting difference spectrum against pure water.

It is apparent from the rows 1, 3 and 5 in Fig 2, that the general structure of the low-frequency region remains unchanged upon addition of the molecules. It is still dominated by quasi-elastic scattering, presenting itself in a Lorentzian line-shape centered at 0 cm^{-1} and a second smaller feature centered at roughly 180 cm^{-1}, which is a well-known collective feature of water [2,17,18]. This second feature can be attributed to a restricted translation of water molecules along a neighboring hydrogen-bonded water molecule, or a O-O stretching vibration along a O···H-O hydrogen bond. Not clearly visible, but also known from literature (and visible in the difference spectra), a second band at ca. 50 cm^{-1} is also contributing to the signal that corresponds to a transversal translation or bending vibration [2,17,18]. For glycine this differs starkly from the low-frequency spectrum in solid form exhibiting several sharp bands, which cannot be found in dissolved form, as no crystal structure is present.

However, looking at the difference spectra of the various concentrations against pure water, it is apparent that the band structure is influenced slightly by the addition of the molecules. Furthermore, this influence is not the same for all molecules. For glycine and acetone, the difference spectra for the whole region have a strictly negative difference except for the region between –20 and +20 cm^{-1}. The region around the 180 cm^{-1} band is more strongly affected than the 50 cm^{-1} band. This is especially pronounced for acetone, where the influence on the 50 cm^{-1} band is much smaller. For sodium chloride, these two areas also show strong negative difference, but a small positive signal at ca. 100 cm^{-1} is present as well.

As the low-frequency bands are a characteristic feature of ordered structures within water, i.e., hydrogen bonding mediated geometric arrangement, changes to the band structure indicate that the hydrogen bonding environment also changes. Loss of intensity of these bands can, therefore, be related to a loss of order in the structure and changes in the frequency can be related to changes of the geometric arrangement or hydrogen bonding partners. As pure water is a highly ordered liquid, almost solely comprised of tetrahedron-like water clusters [19], a loss of organization is expected due to the addition of all molecules. However, depending on the polarity and proticity of the added molecule, it is expected that the organization is affected differently. While tetrahydrofurane should be almost inert in the scope of hydrogen bonding interaction, the aprotic solvent acetone is a weak hydrogen bond acceptor, the protic molecules glycine and glucose can function as hydrogen bond acceptors and donors, and the acids / salts will influence the geometry by changing pH value and ion strength of the solution.

These known attributes in general correlate well with the observed spectra, Fig 2. The apparent disorganization based on the loss of intensity is largest for acetone, slightly smaller for glycine, and very small

for glucose. Positive signals can be seen for sodium chloride and hydrogen chloride, indicating significant rearrangement into a different geometry with a characteristic frequency of ca. 100 cm^{-1}. Only the molecules tetrahydrofurane and acetic acid do not fit with this overall trend. Tetrahydrofurane shows a relatively low change to the overall structure of the low-frequency region, while acetic acid shows behavior similar to acetone, which does not immediately conform to its very polar, protic character and formation of strong hydrogen bonds with water. For tetrahydrofurane the reason for this small change could be, that it does not participate in the hydrogen bonding structure of water and thus does not change its geometry. This means that in the relatively small concentrations investigated here, no major change in the ordered structure of water can be observed as the low amount of tetrahydrofurane molecules only cause minor local changes.

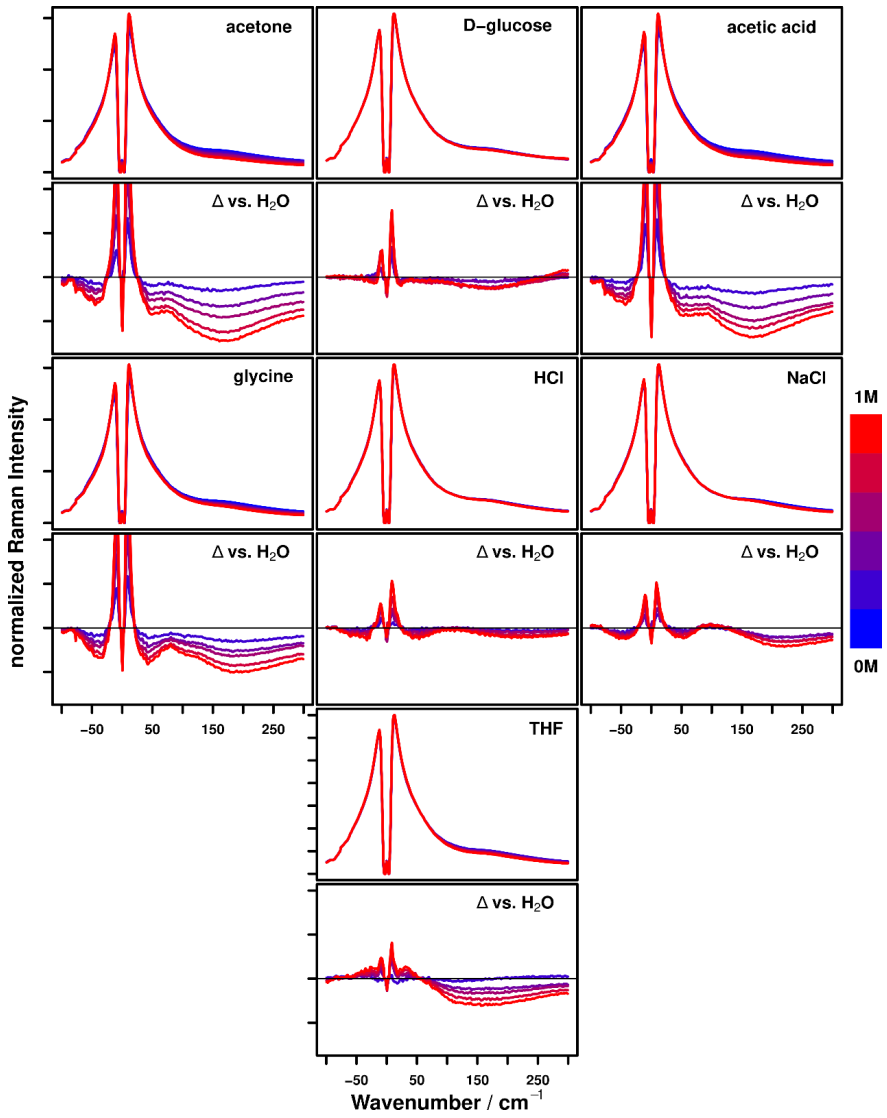

Fig 2. Raman spectra of acetone, D-glucose, acetic acid, glycine, hydrochloric acid, sodium chloride and tetrahydrofurane dissolved in water in concentrations ranging from 0 to 1M and the respective difference spectra against pure water.

For acetic acid, an explanation might be the formation of highly ordered geometric structures by itself. Ultrasonic investigations into the reverse system (acetic acid diluted with a small amount of water), have previously shown loss of organization in this case, as water and acetic acid molecules compete in the dynamic hydrogen bonding process [20]. It is feasible to assume that this behavior could also be present in the system investigated here: The competition of the small amount of acetic acid molecules in the hydrogen bonding system is significantly reducing the degree of organization. However, its concentration is not high enough to form stable geometric structures, that would cause bands in the low frequency spectrum.

3.2 Two-Dimensional Correlation Spectroscopy

Two-dimensional correlation spectroscopy (2DCOS) is a powerful analytical technique used to study complex molecular systems and to extract detailed information about their molecular interactions and dynamics [21,22]. It recovers the correlation function of a set of spectra recorded under external perturbation and can thus be used to investigate if observed changes in a data set are related [23]. It can be used to reveal if changes are (a) correlated, meaning they stem from the same underlying physical process and (b) if they are correlated without a phase-shift (synchronously, i.e., happen with the same rate) or with a phase-shift (asynchronously, i.e., happen with different rates). In highly convolved bands like the ones frequently observed in the low-wavenumber region of a low-frequency Raman spectrum, this can help deconvolving bands, as long as they happen with different rates and thus increase the effective spectral resolution of the measurement.

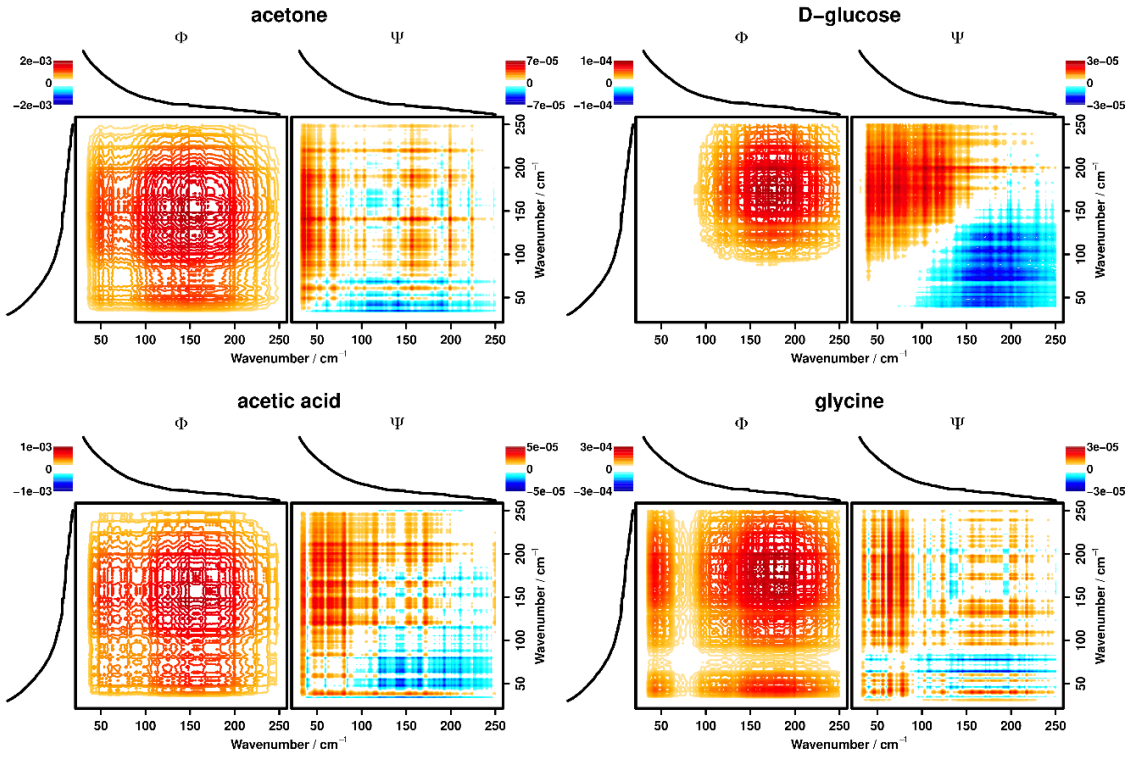

Fig 3. Two-dimensional low-frequency Raman spectra of aqueous solutions of acetone, D-glucose, acetic acid and glycine in concentrations of 0 to 1M (0.1M steps) in the wavenumber region between 20 and 250 cm^{-1}. The pure water spectrum was used as the reference spectrum for calculation of the maps.

In this study, we employed 2DCOS to further analyze the spectral changes discussed in the previous section. It allows for a more unbiased analysis of the spectral changes induced by adding the substances to water, as the resulting signals are based on well-defined mathematical concepts and not just the interpretation of the viewer. Furthermore, it should allow to show, if the changes to the spectra happen in a single process or if multiple processes play a role in modifying the band structure. The resulting 2DCOS maps can be seen in Figs 3 and 4.

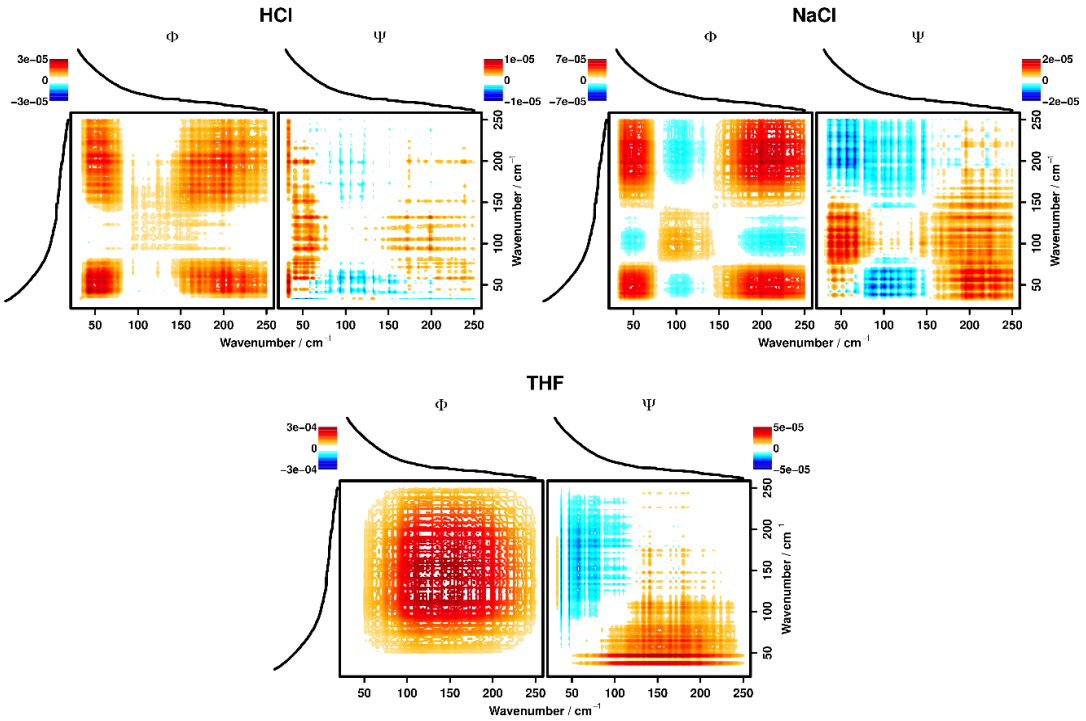

Fig 4. Two-dimensional low-frequency Raman spectra of aqueous solutions of hydrochloric acid, sodium chloride and tetrahydrofurane in concentrations of 0 to 1M (0.1M steps) in the wavenumber region between 20 and 250 cm^{-1}. The pure water spectrum was used as the reference spectrum for calculation of the maps.

Again, significant differences between the different species can be seen in the 2DCOS maps. For most of the species, the synchronous (Φ) map shows strictly positive signals, meaning (according to Noda's first rule) that all signals in the spectrum change in the same direction. The only exception here is sodium chloride, where negative signals can be seen around 100 cm^{-1}, which means (according to Noda's second rule) that this spectral band shows a change in a different direction compared to the rest of the spectrum. This is consistent with the observations made in the previous section on the difference spectra, where a small positive signal could be seen in the same region for sodium chloride.

Similar to sodium chloride, glycine and especially hydrochloric acid show a different pattern along that 100 cm^{-1} band. For hydrochloric acid, almost no correlation intensity can be observed, while for glycine it is at least significantly lower than in the rest of the map, indicating a smaller decrease in intensity here. These substances, therefore, all seem to cause the appearance of a new species, which causes a signal around 100 cm^{-1} to varying degrees. For sodium chloride, the signal of this new species is strong enough to more than recover the loss in intensity. For glycine and hydrochloric acid, it at least significantly decreases the loss of intensity in this region.

The synchronous maps for D-glucose and tetrahydrofurane furthermore differ from those for acetone and acetic acid: while the latter two show a positive signal spanning the whole region between 25 and 250 cm^{-1}, the changes for D-glucose and tetrahydrofurane seem to be restricted to the higher wavenumber region above 100 cm^{-1} for glucose and 50 cm^{-1} for tetrahydrofurane. This indicates that those species have a stronger effect on one of the two hydrogen bonding associated vibrations discussed in the previous section. As discussed previously, this vibration of higher energy is assigned to oxygen vibrations in (almost) linear hydrogen bonds [2], while the lower energy vibration is associated with bending of hydrogen bonds which does not require perfectly linear hydrogen bond geometry. Thus D-glucose and tetrahydrofurane selectively reduce the number of linear hydrogen bonds.

For D-glucose, molecular mechanics calculations have shown, that the oxygen atoms in glucose are not all equally coordinated by water, but the number of coordinating water molecules range from 0.6 to almost 1.8 [24]. This means that not all hydrogen bonds can be perfectly linear, as steric effects will lead to repulsion of the water molecules. This could explain the higher reduction in intensity of the band centered at 180 cm^{-1} compared to the less geometry sensitive band around 50 cm^{-1}. A similar effect was found in a quantum chemistry study for tetrahydrofurane when studying the structures of $THF{\cdot}(H_2O)_{1-10}$ [25]. For $THF{\cdot}(H_2O)_{>2}$, more than one water molecule will form a weak hydrogen bond with the oxygen atom, which leads to the formation of non-linear hydrogen bonds, similar to D-glucose. The same explanation can presumably be applied here as well. The comparatively smaller restriction for tetrahydrofurane, which still shows correlation signals at 50 cm^{-1}, can be explained by the comparatively weaker hydrogen bonds as well as by the fact, that the number of hydrogen bonding sites is much larger for glucose than for tetrahydrofurane.

Besides the synchronous maps discussed until now, the most powerful features of 2DCOS are the asynchronous (Ψ) maps. Compared to the simple analysis of the difference spectra or just analyzing the synchronous maps, asynchronous maps contain additional information regarding the order of changes, which can offer further insight into the systems. For acetone, glycine and acetic acid, no clear structure is apparent in the asynchronous maps – small regions of positive and negative intensity alternate with not clear relation to the signals in their respective synchronous maps. These alternations are typical for asynchronous maps dominated by noise, so that no asynchronicity could be detected for these species.

Glucose and tetrahydrofurane, while sharing many similarities in their synchronous correlation maps differ strongly in their asynchronous maps. While glucose features a positive region between (50, 100) and (150, 250) cm^{-1} (above the main diagonal), this region is negative for tetrahydrofurane. According to Noda's third rule, this means that for D-glucose the lower wavenumber region changes faster than the high wavenumber region and vice-versa for tetrahydrofurane. However, in both cases most of the asynchronous intensity is in a region where no synchronous correlation is apparent, and thus cannot be interpreted. Presumably most of this intensity stems from correlation with changes to the central feature around 0 cm^{-1}, i.e., quasi-elastic scattering which shows residual intensity over the whole spectral range. This should, therefore, not be related to the hydrogen bonding structure of the water in the respective solutions.

However, for hydrochloric acid, and especially for sodium chloride, the asynchronous correlation spectrum gives further insight into the physicochemical changes of the solutions. For sodium chloride negative asynchronous correlation intensity can be seen in the triangle between (0, 0), (100, 100) and (150, 0) cm^{-1} and positive intensity between (250, 0), (150, 150), (250, 200) cm^{-1} below the main diagonal (cf. Fig 4, top-right). The first feature of negative asynchronous correlation intensity overlaps well with the synchronous cross-peak of the band around 50 cm^{-1} and the (new) band at around 100 cm^{-1}, which is also negative. According to Noda's fourth rule, this therefore means that the new band at 100 cm^{-1} starts to appear before significant decrease of the intensity at 50 cm^{-1} happens. On the contrary, the second feature which overlaps well with the synchronous cross-peak of the band around 180 cm^{-1} and the (new) band at around 100 cm^{-1}, shows that the new band occurs after significant decrease of intensity happens in the high wavenumber region. For hydrochloric acid, the general structure of the asynchronous map in this region is very similar to sodium

chloride, although no synchronous cross-peaks can be observed due to the smaller intensity increase of the new band.

These observations once again point to a decoupled influence of the dissolved molecules on the two hydrogen bonding associated bands of water, as has been discussed above for the synchronous 2DCOS maps of D-glucose and tetrahydrofurane. However, in this case the intensity of both bands decreases, but not at the same time. For low concentrations of the substances, mainly the geometry of the hydrogen bonding structure seems to be affected in a way that reduces the number of linear hydrogen bonds and thus the intensity of the O-O stretching vibration at 180 cm^{-1}. Only for higher concentrations is the less geometry dependent band at 50 cm^{-1} affected and its intensity decreases. Interestingly, the observed new signal at 100 cm^{-1} appears before this decrease. This can be explained by a gradual transition from a stable form with a signal located at 50 cm^{-1} to a new form with the signal located at 100 cm^{-1}. In this case, it is well known in literature that correlation patterns like the ones observed here can be seen [26]. This gradual transition is likely, as the influence on the hydrogen bonding structure in this case should be exclusively electrostatic. Therefore, the position of the band is directly related to the ion strength of the solution. The transition thus directly depends on the concentration of sodium chloride [26].

The fact that the correlation patterns for hydrochloric acid are remarkably similar to the patterns observed for sodium chloride furthermore points to the fact that the protons of the hydrochloric acid do not actively participate in the hydrogen bonding. Instead, like sodium chloride, it only influences the hydrogen bonding environment *via* electrostatic interactions of the dissolved ions. This mechanistic insight can only be seen by looking at the 2DCOS maps and thus demonstrates the power of 2DCOS for the analysis of the low-frequency region.

4 Conclusion

To conclude, this paper presents a systematic study investigating the effect of dissolving small molecules and salts ranging from relatively apolar to very polar in water on the low-frequency region of the Raman spectrum. For all species, no characteristic signals of the dissolved molecules could be found in concentrations of 1M, even for larger molecules like D-glucose. However, all molecules can indirectly be detected by changes in the low-frequency spectrum of water, which is mainly governed by the hydrogen bonding structure. The observed changes are the result of a dis- or reorganization of the structure of liquid water due to interaction with the dissolved molecules and can be correlated with physicochemical properties of the respective molecules.

Employing two-dimensional correlation spectroscopy (2DCOS) it was furthermore possible to reveal more detailed mechanistic details of the interaction of the molecules with water, which showed that the two types of hydrogen bonding related bands in the low-frequency region are neither necessarily influenced to the same degree nor at the same time.

On one hand, the presented results demonstrate the power of low-frequency Raman to investigate weak interactions of molecules also in liquid state by investigating changes of the band originating from vibrations or librations associated with the interaction. On the other hand, given a sufficiently large library of investigated model systems, it might be possible to use low-frequency Raman to indirectly detect species dissolved in water or other systems by comparing recorded low-frequency spectra with references.

References

1. Yarwood J, Spectroscopic studies of intermolecular forces in dense phases, *Annual Reports Section C* (*Physical Chemistry*), 76(1979)99–130.
2. Nielsen O F, Low-frequency spetroscopic studies of interactions in liquids, *Annual Reports Section C* (*Physical Chemistry*), 90(1993)3–44.

3. Bērziņš K, S. J. Fraser-Miller S J, Recent advances in low-frequency Raman spectroscopy for pharmaceutical applications, Gordon K C, *Int J Pharm*, 592(2021)120034; doi.org/10.1016/j.ijpharm.2020.120034.
4. Ueno Y, Ajito K, Analytical terahertz spectroscopy, *Anal Sci*, 24(2008)185–192.
5. Shuang B, Wang C X, Xia L, Xu B, Zhang S L, Stray light in low wavenumber Raman spectra and secondary maxima of grating diffraction, *J Raman Spectrosc*, 42(2011)2149–2153.
6. Ivanda M, Babocsi K, Dem C, Schmitt M, Montagna M, Kiefer W, Low-wave-number Raman scattering from CdS_xSe_{1-x} quantum dots embedded in a glass matrix, *Phys Rev B*, 67(2003)235329; doi.org/10.1103/PhysRevB.67.235329.
7. Carriere J T A, Havermeyer F, Ultra-low frequency Stokes and anti-Stokes Raman spectroscopy at 785 nm with volume holographic grating filters, Proc SPIE 8219, Biomedical Vibrational Spectroscopy V: Advances in Research and Industry, 821905, 2012.
8. Heyler R A, Carriere J T A, Havermeyer F, THz-Raman: accessing molecular structure with Raman spectroscopy for enhanced chemical identification, analysis, and monitoring, Proc SPIE 8726, Next-Generation Spectroscopic Technologies VI, 87260J, 2013.
9. Mariotto G, Montagna M, Viliani G, Campostrini R, Carturan G, Low-frequency Raman scattering in thermally treated silica gels: observation of phonon-fracton crossover, *J Phys C: Solid State Physics*, 21(1988)L797; doi.10.1088/0022-3719/21/22/005.
10. Kostić R, Aškrabić S, Dohčević-Mitrović Z, Popović Z V, Scattering from CeO_2 nanoparticles, *Appl Phys A*, 90(2008)679–683.
11. Holomb R, Mitsa V, Johansson P, Veres M, Boson peak in low-frequency Raman spectra of As_xS_{100-x} glasses: nanocluster contribution, *Phys Status Solidi C*, 7(2010)885–888.
12. Noda I, Roy A, Carriere J, Sobieski B J, Chase D B, Rabolt J F, Two-dimensional Raman correlation spectroscopy study of poly [(R)-3-hydroxybutyrate-co-(R)-3-hydroxyhexanoate] copolymers, *Appl Spectrosc*, 71(2017)1427–1431.
13. Larkin P J, Dabros M, Sarsfield B, Chan E, Carriere J T, Smith B C, Polymorph Characterization of Active Pharmaceutical Ingredients (APIs) Using Low-Frequency Raman Spectroscopy, *Appl Spectrosc*, 68(2014)758–776.
14. Damle V H, Aviv H, Tischler Y R, Identification of Enantiomers Using Low-Frequency Raman Spectroscopy, *Anal Chem*, 94(2022)3188–3193.
15. Suresh S J, Satish A V, Choudhary A, Influence of electric field on the hydrogen bond network of water, *J Chem Phys*, 124(2006)074506; doi.org/10.1063/1.2162888.
16. Hniopek J, Schmitt M, Popp J, Bocklitz T, PC 2D-COS: A Principal Component Base Approach to Two-Dimensional Correlation Spectroscopy, *Appl Spectrosc*, 74(2020)460–472.
17. Padró J A, Martı J, An interpretation of the low-frequency spectrum of liquid wateŕ, *J Chem Phys*, 118(2003)452; doi.org/10.1063/1.1524619.
18. Mizoguchi K, Hori Y, Tominaga Y, Study on dynamical structure in water and heavy water by low-frequency Raman spectroscopy, *J Chem Phys*, 97(1992)1961; doi.org/10.1063/1.463133.
19. Kusalik P G, Svishchev I M, The spatial structure in liquid water, *Science*, 265(1994)1219–1221.
20. Corsaro R D, Atkinson G, Ultrasonic Investigation of Acetic Acid Hydrogen Bond Formation. II Acetic Acid–Water Solutions, *J Chem Phys*, 55(1971)1971; doi.org/10.1063/1.1676336.
21. Noda I, Generalized two-dimensional correlation method applicable to infrared, Raman, and other types of spectroscopy, *Appl Spectrosc*, 47(1993)1329–1336.
22. Noda I, Dowrey A E, Marcott C, Story G M, Ozaki Y, Generalized two-dimensional correlation spectroscopy, *Appl Spectrosc*, 54(2000)236A–248A.
23. Noda I, Close-up view on the inner workings of two-dimensional correlation spectroscopy, *Vib Spectrosc*, 60(2012)146–153.
24. Te J A, Tan M.-L, Ichiye T, Solvation of glucose, trehalose, and sucrose by the soft-sticky dipole–quadrupole–octupole water model, *Chem Phys Lett*, 491(2010)218–223.
25. Liu J, Yan Y, Yan Y, Zhang J, Tetrahydrofuran (THF)-Mediated Structure of $THF{\cdot}(H_2O)_{n=1-10}$: A Computational Study on the Formation of the THF Hydrate, *Crystals*, 9(2019)73; doi.org/10.3390/cryst9020073.
26. Czarnecki M A, Interpretation of two-dimensional correlation spectra: science or art?, *Appl Spectrosc*, 52(1998)1583–1590.

[*Received*: 15.02.2023; *revised recd*: 26.02.2023; *accepted*: 28.02.2023]